Shielding Effect of a Thick Screen with Corrugations

Matteo Albani, *Member, IEEE*, Peter Piazzesi, Filippo Capolino, *Member, IEEE*, Stefano Maci, *Member, IEEE*, and Roberto Tiberio, *Fellow, IEEE*

***Abstract*— The shielding effectiveness of a corrugated thick screen is theoretically and experimentally investigated. This screen consists of a half-plane of finite thickness in which corrugations are etched on the smaller side. This structure provides a significant attenuation in the shadow region for both polarizations of the incident field; thus, it can be effectively used for protecting apparatuses from radiating interference as well as for decoupling nearby operating antennas. The shielding properties of the screen are described by a high-frequency formulation that involves closed-form expressions. An experimental setup at X band has been arranged to test the effectiveness of a corrugated screen; the field in the shadow region is compared with that of a screen without corrugations. The experimental results compare very well with those obtained by the high-frequency expressions.**

***Index Terms*—Diffraction, high-frequency, shielding.**

I. Introduction

OVERCROWDED platforms are often subjected to electromagnetic coupling between antennas and/or apparatuses operating close to each other. The engineering solutions for reducing interference and electromagnetic compatibility problems are of increasing importance, particularly for satellite environments. One of the most simple, but effective ways to reduce the radiating interference is to introduce barriers or fins between the two coupled systems. This solution can be also useful in reducing radiating interference in earth satellite stations [1]. In particular, interference that arises from microwave links operating at the same frequency often arrives from directions close to the horizon; they may sometimes be attenuated by diffraction losses at natural barriers occurring in terrain propagation. In other cases, introducing artificial shielding barriers may greatly alleviate these problems.

The simplest canonical model of a barrier for interference protection is a perfectly conducting thick screen of a semi-infinite extent. When the source and the observer are optically shadowed, a field coupling still occurs due to double diffraction (DD) mechanisms at the two nearby parallel edges of the screen. Consequently, its shielding effectiveness significantly depends upon the thickness and the polarization of the incident field. In particular, when the incident electric field is parallel to the edges (TM$_z$ pol, soft boundary condition), the diffracted field into the shadow region is very weak since the first-order diffracted field is short circuited by the conducting portion between the two edges. Then, the second-order diffraction essentially consists in a slope effect that becomes weaker as the thicknesses increases.

On the other hand, when the incident electric field is perpendicular to the edges (TE$_z$ pol, hard boundary condition), a stronger field propagates in shadow region because the first-order diffracted field does not vanish between the two edges. This results in a poor shielding. In order to improve the shielding effectiveness for this polarization, one can etch in the face joining the two edges a quarter of a wavelength deep corrugations, with a periodicity small with respect to the wavelength. For such configurations, the surface at the top of the corrugations may be appropriately modeled as a perfectly magnetic conducting (PMC) surface for the TE$_z$ pol and a perfectly electric conducting (PEC) surface for the TM$_z$ pol; thus, an artificially soft boundary condition (BC) is obtained [2], that leads to a similar behavior of the field for *both polarizations*.

In this paper, the shielding effectiveness of a thick corrugated screen of semi-infinite extent is investigated. In particular, in Section II, a brief description of the phenomena is given and a closed-form high-frequency solution is presented to calculate singly and doubly diffracted field contributions from the edges of the screen. In Section III, an X-band experimental setup is described; in Section IV, numerical and experimental results are presented and compared.

II. High-Frequency Solution

The cross section of the thick screen is shown in Fig. 1 in the cases of smooth top face and corrugated top face. Two parallel axes are defined along the two edges (normal to the plane of the paper and outcoming from it), and a cylindrical coordinate system (ρ_i, ϕ_i, z_i) is introduced at each edge $i = 1, 2$; $n_i\pi$ denotes the exterior wedge angle at each edge and ℓ the thickness of the screen. In most practical cases $n_i = 3/2$. A spherical incident either TMz or TE$_z$ field is assumed. When the TE$_z$ ray propagates along the corrugated surface after diffracting at the trailing edge, it excites TEM modes inside the corrugations. The H-field tangent to the top face is short circuited by the $\lambda/4$ deep corrugations, thus yielding a vanishing grazing ray. In our high-frequency treatment, an artificially soft BC model is used at the top of the corrugations; i.e., PEC for TM$_z$ and PMC for TE$_z$ polarization. This assumption requires that both the source point $P' \equiv (\rho_i', \phi_i', z_i' = 0)$ and the observation point

Manuscript received July 8, 1996; revised April 28, 1998.

The authors are with the College of Engineering, University of Siena, Siena, 53100 Italy.

Publisher Item Identifier S 0018-9375(98)06193-6.

$P \equiv (\rho_i, \phi_i, z_i = 0)$ lie on the same plane perpendicular to the screen. Indeed, for oblique incidence, more sophisticated anisotropic BC are needed. The total field at the observation point P is described as the sum of the following contributions

$$\vec{E}^t = \vec{E}^{\mathrm{GO}} + \vec{E}^d + \vec{E}^{dd} \tag{1}$$

in which $\vec{E}^{\mathrm{GO}}$ is the incident plus reflected geometrical optics (GO) field, $\vec{E}^d$ denotes singly diffracted ray-field contributions and $\vec{E}^{\mathrm{dd}}$ doubly diffracted field contributions. Each contribution may or may not exist, depending on both the incidence and observation aspects as can be easily inferred from simple ray tracing. Singly diffracted contributions are represented as

$$\vec{E}^d = \vec{E}_1^d + \vec{E}_2^d \tag{2}$$

where $\vec{E}_1^d(\vec{E}_2^d)$ is the ray-field singly diffracted at edge 1 (edge 2) that is calculated by

$$\vec{E}_1^d = \vec{E}^i(Q_1) \cdot \underline{\underline{\mathcal{D}}}_1 \sqrt{\frac{\rho_1'}{\rho_1(\rho_1 + \rho_1')}}\, e^{-jk\rho_1} \tag{3}$$

where $\vec{E}^i(Q_1)$ is the incident field at the diffraction point Q_1 on the edge 1 and the diffraction dyad is defined as

$$\mathcal{D}_1 = \hat{z}_1\hat{z}_1 D_1^s - \hat{\phi}_1'\hat{\phi}_1 D_1^{a,\,h}. \tag{4}$$

Here and henceforth, k denote the wavenumber and a harmonic $e^{j\omega t}$ time dependence is assumed and suppressed. In (4), D_1^s and D_1^h are ordinary diffraction coefficients predicted by the uniform theory of diffraction (UTD) [3] that apply to perfectly conducting wedges in the TM$_z$ and TE$_z$ case, respectively; D_1^a is the UTD diffraction coefficient for TE$_z$ illuminated wedge with corrugations on the face $\phi_1 = 0$ [4], [5]. Here, the spreading factor and the distance parameter have been suitably modified to account for the spherical incident wavefront. This leads to

$$\begin{aligned} D_1^a = -\frac{1}{2n_1\sqrt{2\pi jk}} \Bigg\{ &\left[\csc\left(\frac{\pi + \Phi^-}{2n_1}\right) F[kLa^+(\Phi^-)] \right. \\ &\left. + \csc\left(\frac{\pi - \Phi^-}{2n_1}\right) F[kLa^-(\Phi^-)] \right] \\ &- \left[\csc\left(\frac{\pi + \Phi^+}{2n_1}\right) F[kLa^+(\Phi^+)] \right. \\ &\left. + \csc\left(\frac{\pi - \Phi^+}{2n_1}\right) F[kLa^-(\Phi^+)] \right] \Bigg\} \end{aligned} \tag{5}$$

in which

$$F(y) = 2j\sqrt{y}e^{jy}\int_{\sqrt{y}}^{\infty} e^{-jt^2}\,dt; \quad -\frac{3\pi}{2} < \arg(y) \le \frac{\pi}{2} \tag{6a}$$

is the UTD transition function, whose arguments involve

$$\begin{aligned} L &= \frac{\rho_1\rho_1'}{\rho_1 + \rho_1'}, \\ \Phi^{\pm} &= \phi_1 \pm \phi_1', \\ a^{\pm}(\Phi) &= 2\cos^2\left(\frac{2n_1\pi N^{\pm} - \Phi}{2}\right) \end{aligned} \tag{6b}$$

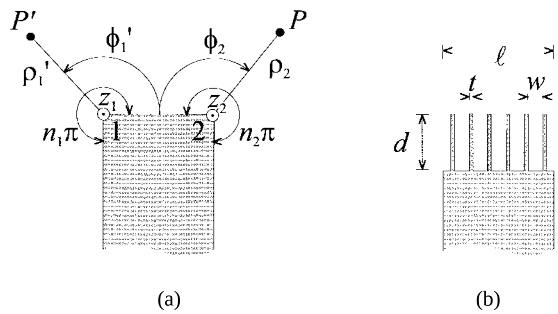

Fig. 1. Geometry and reference systems. (a) Smooth screen. (b) Corrugated screen.

with $N^{\pm}$ denoting the integer that most nearly satisfies $N^{\pm} = (\pm\pi + \Phi)/(2\pi n_1)$. Note that the expression of D_1^a is identical to that of the ordinary UTD soft diffraction coefficient D_1^s, except for the cosecant functions that replaces the typical cotangent functions. The analogous contribution E_2^d is easily obtained by substituting subscript 1 with 2.

Doubly diffracted ray-field contribution E^{dd} is represented as

$$E^{dd} = E_{12}^{dd} + E_{21}^{dd} \tag{7}$$

where $\vec{E}_{ij}^{dd}$ is the doubly diffracted contribution that arises from edge j after diffracting at edge i. The contribution $\vec{E}_{12}^{dd}$ is obtained from the formulation presented in [6], [7] that is relevant to a line source illumination, by introducing a suitable modification in the spreading factor and in the distance parameters. This leads to

$$\vec{E}_{12}^{dd} = \vec{E}^i(Q_1) \cdot \underline{\underline{\mathcal{D}}}_{12} \sqrt{\frac{\rho_1'}{\rho_2\ell(\rho_1' + \ell + \rho_2)}}\, e^{-jk(\ell + \rho_2)} \tag{8}$$

where the diffraction dyad is defined as

$$\underline{\underline{\mathcal{D}}}_{12} = \hat{z}_1\hat{z}_1 D_{12}^s + \hat{\phi}_1'\hat{\phi}_2 D_{12}^{a,\,h}. \tag{9}$$

In (9), D_{12}^s denotes the DD coefficient for soft BC that applies to TM$_z$ pol, while D_{12}^h and D_{12}^a denote the DD diffraction coefficients for the hard and the artificially soft cases, respectively; these latter apply to the TE$_z$ pol for smooth and corrugated screen, respectively. They are expressed as

$$\begin{aligned} D_{12}^h = \frac{1}{4\pi jk} \cdot \sum_{p,\,q=1}^{2} &\frac{(-1)^{p+q}}{n_1 n_2} \cot\left(\frac{\Phi_1^p}{2n_1}\right) \\ &\cdot \cot\left(\frac{\Phi_2^q}{2n_2}\right) \cdot \tilde{T}(a_p,\, b_q,\, w) \end{aligned} \tag{10}$$

$$\begin{aligned} D_{12}^a = \frac{-1}{16\pi k^2\ell} \cdot \sum_{p,\,q=1}^{2} &\frac{(-1)^{p+q}}{(n_1 n_2)^2} \frac{\cos\left(\frac{\Phi_1^p}{2n_1}\right)}{\sin^2\left(\frac{\Phi_1^p}{2n_1}\right)} \\ &\cdot \frac{\cos\left(\frac{\Phi_2^q}{2n_2}\right)}{\sin^2\left(\frac{\Phi_2^q}{2n_2}\right)} \cdot \tilde{\tilde{T}}(a_p,\, b_q,\, w) \end{aligned} \tag{11}$$

and

$$D_{12}^{s} = \frac{-1}{16\pi k^2 \ell} \cdot \sum_{p,\,q=1}^{2} \frac{(-1)^{p+q}}{(n_1 n_2)^2} \csc^2\left(\frac{\Phi_1^p}{2n_1}\right) \cdot \csc^2\left(\frac{\Phi_2^q}{2n_2}\right) \cdot \tilde{\tilde{T}}(a_p, b_q, w) \tag{12}$$

in which $\Phi_1^p = \phi_1' + (-1)^p \pi$ and $\Phi_2^q = \phi_2 + (-1)^q \pi$. Equations (10)–(12) involve the transition functions

$$\begin{aligned}\tilde{T}(a, b, w) &= \frac{2\pi jab}{\sqrt{1-w^2}}\left[\mathcal{G}\left(a, \frac{b+wa}{\sqrt{1-w^2}}\right) + \mathcal{G}\left(b, \frac{a+wb}{\sqrt{1-w^2}}\right)\right. \\ &\quad \left. + \mathcal{G}\left(a, \frac{b-wa}{\sqrt{1-w^2}}\right) + \mathcal{G}\left(b, \frac{a-wb}{\sqrt{1-w^2}}\right)\right]\end{aligned} \tag{13}$$

and

$$\begin{aligned}\tilde{\tilde{T}}(a, b, w) &= \frac{-4\pi(ab)^2}{w\sqrt{1-w^2}}\left[\mathcal{G}\left(a, \frac{b+wa}{\sqrt{1-w^2}}\right) + \mathcal{G}\left(b, \frac{a+wb}{\sqrt{1-w^2}}\right)\right. \\ &\quad \left. - \mathcal{G}\left(a, \frac{b-wa}{\sqrt{1-w^2}}\right) - \mathcal{G}\left(b, \frac{a-wb}{\sqrt{1-w^2}}\right)\right]\end{aligned} \tag{14}$$

where $\mathcal{G}$ is the generalized Fresnel integral (GFI) defined as in [8] where a very simple algorithm is suggested for its numerical computation.

The distance parameters in the transition functions are

$$\begin{aligned} a_p &= \sqrt{2k\,\frac{\rho_1'\ell}{\rho_1'+\ell}}\,\sin\left(\frac{\Phi_1^p - 2n_1 N^p \pi}{2}\right) \\ b_q &= \sqrt{2k\,\frac{\rho_2\ell}{\rho_2+\ell}}\,\sin\left(\frac{\Phi_2^q - 2n_2 N^q \pi}{2}\right)\end{aligned} \tag{15}$$

and

$$w = \sqrt{\frac{\rho_1'\rho_2}{(\rho_1'+\ell)(\ell+\rho_2)}} \tag{16}$$

where N^p and N^q are the integers that most nearly satisfy the relations $N^p = \Phi_1^p/(2n_1\pi)$ and $N^q = \Phi_2^q/(2n_2\pi)$, respectively.

The expression for E_{21}^{dd} is easily obtained by interchanging 1 and 2 in (8)–(16).

III. Experimental Setup

An experimental setup at 8.2 GHz in an anechoic chamber has been arranged in order to test the shielding effectiveness of a corrugated screen (Fig. 2). A square corrugated screen 1 m $\times$ 1 m has been constructed by two copper sheets supported by a frame of wood. On the top side, an aluminum rod is mounted, which is corrugated on one side and smooth on the other, so that by simply reversing it, both corrugated and smooth thick screens are obtained. This permits the comparison between the performances of these two different structures at the two polarizations. The space w between the teeth and their thickness t are $w = 4$ mm (0.11λ) and $t = 1$ mm (0.03λ), respectively [Fig 1(b)]. The depth of the corrugations is $d = 91.4$ mm ($\lambda/4$) and the thickness of the rod is $\ell = 30$ mm (0.82λ), which contains six teeth. The transmitting and the receiving antennas are pyramidal horns with 5.5 cm $\times$ 7.5 cm and 7.5 cm $\times$ 7.5 cm apertures, respectively. The fundamental TE_{10} mode, with a quasiuniform phase distribution on the aperture is obtained in both horns, so that the phase center can be assumed on the aperture plane. The transmitting horn is connected via a rectangular X-band waveguide to a TWT amplifier, fed by a HP8341B synthesized sweeper. A twist is used for changing the polarization of the transmitting antenna. The receiving antenna is connected via a 50-Ω coaxial cable to a HP8566B spectrum analyzer.

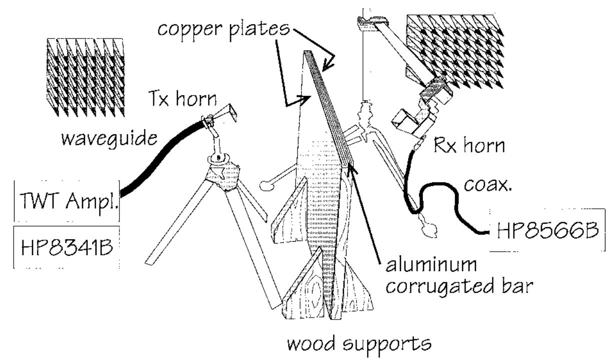

Fig. 2. Experimental setup.

The transmitting horn has been placed at 10λ (36.6 cm) from the trailing edge, so that the edge is in the far-field region of the antenna. The receiving antenna is moved at a constant distance (10λ) from the second edge, from the lit to the shadow region. The angular scan of the receiving horn starts in the lit region at about 10° above the incidence shadow boundary of the leading edge, and stops at 30° from the shadowed face of the screen. In order to avoid gain variations, the aperture of the receiving horn has been maintained tangent to the scan circle for all the angular positions.

IV. Numerical and Experimental Results

Calculations have been carried out to test the accuracy of the present formulation, as well as to demonstrate the effectiveness of the corrugations in shielding arbitrarily polarized incident fields. In Fig. 3, theoretical and experimental data for the total field are plotted by continuous lines and discrete symbols, respectively. The relevant geometries and observation scans are depicted in the insets. The phase center of the transmitting antenna is placed at $\rho_1' = 10\lambda$ from the leading edge and at 90° [Fig. 3(a)] and 60° [Fig. 3(b)] from the lit face of the screen.

The results relevant to a smooth PEC thick screen in TE_z pol (hard) are plotted by a short-dashed line (numerical) and black squares (experimental). The PEC TM_z (soft) results, are plotted by a long-dashed line (numerical) and white squares (experimental). Results for the corrugated screen in TE_z pol (artificially soft) are plotted by a continuous line (numerical) and black triangles (experimental). Experimental results have also been obtained for corrugated screen in the TM_z pol (white triangles). The latter practically coincide with those for the smooth screen, thus demonstrating that the TM_z pol is almost insensitive to the corrugations—as expected.

The agreement between numerical and experimental results has been found very satisfactory even at grazing illumination

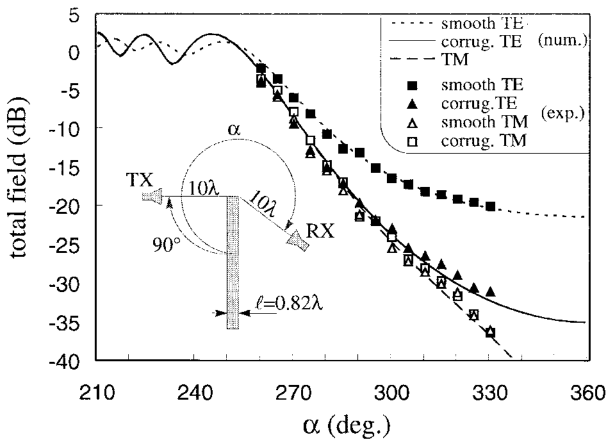

(a)

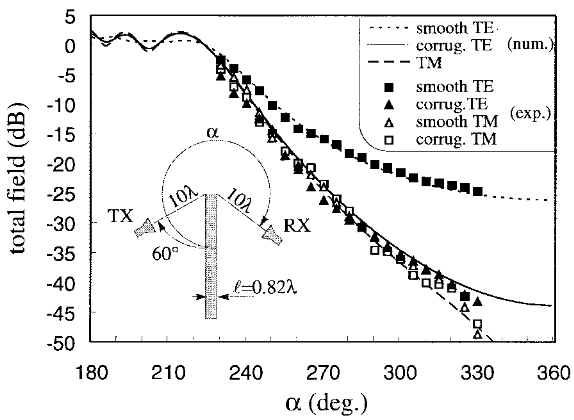

(b)

Fig. 3. Comparison between experimental and high-frequency results in total field amplitude for a screen with thickness $\ell = 0.82\lambda$; dotted line: smooth TE_z (hard); continuous line: corrugated TE_z (artificially soft); dashed line: TM_z (soft case). Transmitting horn located at (a) 90° and (b) 60° from the illuminated face.

[Fig. 3(a)]. It is worth noting that in this case the mathematical description of the physical phenomenon is complicated by the fact that the singly diffracted field exhibits a nonray optical behavior at the second edge, thus requiring the use of the transition functions defined in (13) and (14).

When the receiving antenna gets into the shadow region behind the screen, the artificially soft BC plays an important role, since the total field is dominated by the doubly diffracted field. Indeed, for the TE_z pol the field of the corrugated screen exhibits an attenuation, which is much stronger (more than 10 dB) than that of the smooth screen. This emphasizes that the corrugations provide a strong shielding effect even for TE_z pol, which becomes comparable to that for the TM_z pol. Then, when the receiving antenna approaches the shadowed face, the curves relevant to the soft and artificially soft cases gradually deviate one from the other. This gives evidence to the fact that there the field is mainly influenced by the BC of the shadowed face, as can be inferred from the slope of the two TE_z curves. Nevertheless, the attenuation of the corrugated screen is still several decibels stronger than that of the smooth screen for the same TE_z pol.

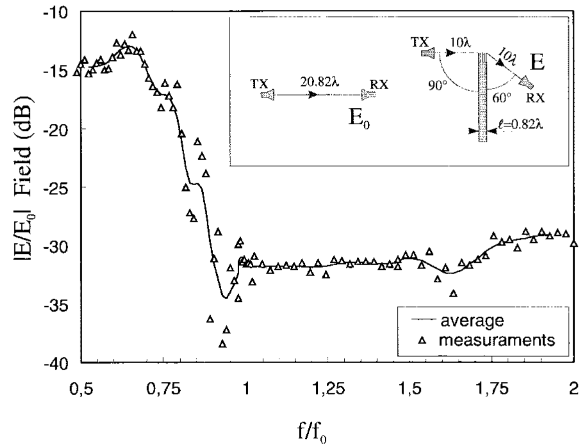

Fig. 4. Amplitude of the field behind corrugated screen as a function of the normalized frequency. Resonant frequency is $f_o = 8.2$ GHz at which the depth of the corrugation is a quarter of a wavelength. △ △ △: experimental results; ______: average.

Measurements have also been carried out for investigating the bandwidth of the shielding effectiveness. The results in Fig. 4 are relevant to the geometry shown in the inset. The data are properly normalized with respect to the field obtained by directly coupling the two antennas at a distance of 20.82λ, which is the same length of the DD ray-path. This permits to avoid that the frequency dependence of the antenna gain may affect the field data. Measurements have been performed from 4 to 16.4 GHz while 8.2 GHz is the design frequency of the corrugations. Different horns have been used to cover the bandwidth. The experimental data are plotted by symbols in Fig. 4 where an averaging continuous line is also shown. An almost flat behavior of the normalized field is found for higher frequencies than the resonant frequency. This is probably due to the fact that the thickness of the screen increases in terms of the wavelength, and this compensates the loss of shielding effectiveness caused by the nonresonant behavior of the corrugations. At variance, at lower frequencies the field increases rapidly (until 20 dB over the attenuation in band). This rapid variation can be explained by observing that at lower frequency, the corrugations model a reactive impedance BC of inductive nature. This kind of BC supports surface waves excitation [9]–[12] so that the loss of shielding effectiveness may be attributed to the diffraction at the second edge of surface waves excited at the first edge.

V. Concluding Remarks

A theoretical and experimental investigation on the shielding effectiveness of a thick corrugated screen has been carried out. It is found that this structure can usefully be employed for decoupling nearby antennas operating in an overcrowded environment, since it provides a strong decoupling for both polarizations of the incident field. The theoretical analysis has been performed by applying a high-frequency solution, which is obtained by modeling the corrugated surface by an artificially soft BC. Experimental data have demonstrated that the screen may also be used at higher frequency with respect to the design frequency; at lower frequencies the properties of the screen rapidly degradates. The electromagnetic model presented here does not allow wide bandwidth description and a more complete analysis involving reactive impedance boundary condition is required, which is presently under progress.

References

[1] S. A. Bokhari, M. Keer, and F. E. Gardiol, "Site shielding of earth-station antennas," *IEEE Antennas Propagat. Mag.*, vol. 37, pp. 7–24, Feb. 1995.

[2] P.-S. Kildal, "Artificially soft and hard surfaces in electromagnetics," *IEEE Trans. Antennas Propagat.*, vol. 38, pp. 1537–1544, Oct. 1990.

[3] R. G. Kouyoumjian and P. H. Pathak, "A uniform geometrical theory of diffraction for an edge in a perfectly conducting surface," *Proc. IEEE*, vol. 62, pp. 1448–1461, Nov. 1974.

[4] S. Maci, R. Tiberio, and A. Toccafondi, "Diffraction coefficient for artificially soft and hard surfaces," *Electron. Lett.*, vol. 30, no. 3, pp. 203–204, Feb. 1994.

[5] M. Leoncini, S. Maci, and A. Toccafondi, "Analysis of the electromagnetic scattering by artificially soft discs," *Proc. Inst. Elect. Eng.*, vol. 142, pt. H, no. 5, pp. 399–404, Oct. 1995.

[6] F. Capolino, M. Albani, S. Maci, and R. Tiberio, "Diffraction from a couple of coplanar, skew wedges," *IEEE Trans. Antennas Propagat.*, vol. 45, pp. 1219–1226, Aug. 1997.

[7] M. Albani, F. Capolino, S. Maci, and R. Tiberio, "Diffraction at a thick screen including corrugations on the top face," *IEEE Trans. Antennas Propagat.*, vol. 45, pp. 277–283, Feb. 1997.

[8] F. Capolino and S. Maci, "Simplified, closed-form expressions for computing the generalized Fresnel integral and their application to vertex diffraction," *Microwave Opt. Tech. Lett.*, vol. 9, no. 1, pp. 32–37, May 1995.

[9] O. M. Bucci and G. Franceschetti, "Electromagnetic scattering by a half plane with two face impedances," *Radio Sci.*, vol. 11, pp. 49–59, Jan. 1976.

[10] R. G. Rojas, "Electromagnetic diffraction of an obliquely incident plane wave field by a wedge with impedance faces," *IEEE Trans. Antennas Propagat.*, vol. 36, pp. 956–970, July 1988.

[11] R. Tiberio, G. Pelosi, G. Manara, and P. H. Pathak, "High frequency scattering from a wedge with impedance faces illuminated by a line source—Part I: Diffraction," *IEEE Trans. Antennas Propagat.*, vol. 37, pp. 212–218, Feb. 1989.

[12] G. Manara, R. Tiberio, G. Pelosi, and P. Pathak "High-frequency scattering from a wedge illuminated by a line source—Part II: Surface waves," *IEEE Trans. Antennas Propagat.*, vol. 41, July 1993.

Matteo Albani (M'95) was born in Florence, Italy, in 1970. He received the Doctor degree (*cum laude*) in electronic engineering from the University of Florence, Italy, in 1994.

From 1994 to 1995, he worked as a Consultant for Ingegneria dei Sistemi (IDS) Pisa, Italy. He is an Instructor at the Department of Information Engineering, University of Siena, Italy. He is currently working in a research program at the University of Siena, Italy, regarding the high-frequency methods for the electromagnetic scattering and diffraction. His research interests also include numerical methods for electromagnetics.

Dr. Albani received a special award for his Laurea thesis work from the University of Florence.

Peter Piazzesi was born in Florence, Italy, in 1969. He received the Doctor degree (*cum laude*) in electronic engineering from the University of Florence, Italy, in 1994.

From 1994 to 1995, he was involved in a research program concerning patch antennas. He served in the Army in 1995 as Technical Officer working on electromagnetic compatibility test and measurements. Since 1996 he has been employed as a Senior Engineer at ENEL (the Italian body for the generation and distribution of the electric power).

Dr. Piazzesi received a special award for his Laurea thesis work from the University of Florence.

Filippo Capolino (S'94–M'97) was born in Florence, Italy, in 1967. He received the Doctor (*cum laude*) (electronic engineering) and the Ph.D. degrees from the University of Florence, Italy, in 1993 and 1997, respectively.

From 1994 to 1996, he was an Instructor at the University of Siena, Italy, where he is currently a Research Assistant. His research interests mainly concern theoretical and applied electromagnetics, with a focus on high-frequency methods for electromagnetic scattering and electromagnetic models of random surfaces.

Dr. Capolino received the 1994 Student Paper Award at the mathematical methods for electromagnetic theory (MMET). In 1996 he won the Raj Mittra Travel Grant for Young Scientists and the "Barzilai" prize for the Best Paper at the National Italian Congress of Electromagnetism (XI RiNEm). In 1997 he was recipient of the Fulbright Fellowship at Boston University, Boston, MA.

Stefano Maci (M'92) was born in Rome, Italy, in 1961. He received the Doctor degree in electronic engineering from the University of Florence, Italy, in 1987.

In 1990, he joined the Department of Electronic Engineering of the University of Florence as Assistant Professor. From 1993 to 1997 he was an Adjunct Professor at the University of Siena, Italy, where he is currently an Associate Professor. In 1997 he was an Invited Professor at the Technical University of Denmark, Copenhagen. His interests are focused on electromagnetic theory, mainly concerning high- and low-frequency methods for antennas and electromagnetic scattering. He has also developed research activity on specific topics concerning microwave antennas, particularly focused on the analysis, synthesis, and design of patch antennas. Since 1996 he has been involved in projects for the European Space Agency regarding electromagnetic modeling.

Dr. Maci received the National Young Scientists "Francini" Award for the Laurea thesis in 1988 and the "Barzilai" prize for the Best Paper at the National Italian Congress of electromagnetism (XI RiNEm) in 1996.

Roberto Tiberio (M'81–SM'83–F'93) was born in Rome in 1946. He received the Doctor degree (*cum laude*) from the University of Pisa, Pisa, Italy, in 1970.

From 1972 to 1993, he was with the Department of Electronic Engineering, University of Florence, Italy, as a Full Professor. In 1993 he joined the University of Siena, Siena, Italy, where he is the Dean of the College of Engineering. Since 1976, he has been collaborating with the Electroscience Laboratory of the Ohio State University, Columbus, where he worked for two years as a Senior Research Assistant and then, periodically, as a Scientific Consultant. His research interests are focused on electromagnetic theory and high-frequency methods, mainly concerning the development and applications of analytic and numerical techniques for antenna design and radar cross section prediction.

Dr. Tiberio is an Italian Delegate of URSI (Commission B).